



Structure and bioactivity of cholestane glycosides from the bulbs of *Ornithogalum saundersiae* Baker

Qing-Wei Chen, Xu Zhang, Ting Gong, Wan Gao, Shuai Yuan, Pei-Cheng Zhang^{**},
Jian-Qiang Kong^{*}

Institute of Materia Medica, Chinese Academy of Medical Sciences & Peking Union Medical College, (State Key Laboratory of Bioactive Substance and Function of Natural Medicines & NHC Key Laboratory of Biosynthesis of Natural Products), Beijing, 100050, China



ARTICLE INFO

Keywords:

Ornithogalum saundersiae baker
Asparagaceae
Cholestane glycosides
Cytotoxicity
Acylated steroidal glycoside

ABSTRACT

Eight undescribed cholestane glycosides named osaundersioside A–H, along with three previously known compounds named osaundersioside I–K were isolated from *Ornithogalum saundersiae* Baker bulbs (Asparagaceae). Their structures were elucidated by extensive spectroscopic analysis and chemical methods. All isolates were evaluated for their cytotoxic activity and inhibitory effects on lipopolysaccharide (LPS)-induced nitric oxide (NO) production. Osaundersioside C was thus determined to exhibit specific cytotoxicity towards MCF-7 cell line with an IC₅₀ value of 0.20 μM, Osaundersioside H exhibited inhibitory effect on NO production in macrophages at the concentration of 10⁻⁵ M, with inhibition rate of 56.81%.

1. Introduction

Ornithogalum saundersiae Baker (Asparagaceae; synonym *Galtonia saundersiae* (Baker) Mart.-Azorín, M.B. Crespo & Juan) is a bulbous plant belonging to the subfamily Scilloideae of the family Asparagaceae (Iguchi et al., 2017a). *O. saundersiae* Baker is native to Africa, and was introduced to other parts of the world as an ornamental plant (Yuan et al., 2018; Liu and Kong, 2018). A systematic phytochemical examination of the bulbs of *O. saundersiae* Baker began in 1992 (Kubo et al., 1992a, 1992b) and led to the discovery of three previously-undescribed acylated cholestane glycosides, including the well-known antitumor molecule OSW-1 (Malabed et al., 2017; Wojtkielewicz et al., 2007). In the interim, many cholesteric compounds have been isolated from this plant, several of which have potent cytotoxic activity against tumor cells (Kubo et al., 1992; Hirano et al., 1996; Kuroda et al., 1993, 1995; 1997, 1999a; 1999b, 2001; Mimaki et al., 1996a, 1996b, 1996c, 1997; Iguchi et al., 2017b). The discovery of these diverse cholestane glycosides, and their associated potent cytotoxic activities suggested that further phytochemical analysis of this plant could be beneficial. Further study resulted in the isolation of eight previously-undescribed compounds designated as osaundersioside A–H (1–8), and three known compounds named osaundersioside I–K (9–11) (Fig. 1). All isolates were evaluated for cytotoxic activity and inhibitory effects on lipopolysaccharide (LPS)-induced nitric oxide (NO) production.

2. Results and discussion

2.1. Structure elucidation

Osaundersioside A (1) was obtained as an amorphous solid, and positive-ion high-resolution electrospray mass spectrometry (HRESIMS) resulted in a peak at m/z 925.4797 [M + Na]⁺ (MW 902.4875), which corresponded to a molecular formula of C₄₅H₇₄O₁₈. The [M-146 + Na]⁺ precursor ion peak at m/z 779 fragmented to yield a neutral loss of 146, which indicated the presence of a terminal deoxyhexose moiety in 1. The ¹H-NMR spectrum in pyridine-*d*₅ of 1 displayed two angular methyl proton signals at δ_H 1.02 (s, Me-18) and 1.43 (s, Me-19), two methyl proton signals at an olefinic carbon at δ_H 1.69 (s, Me-26) and 1.71 (s, Me-27), and one secondary methyl proton signal at δ_H 1.28 (d, $J = 7.2$ Hz, Me-21). An additional methyl doublet observed at δ_H 1.73 (d, $J = 5.4$ Hz) was consistent with the presence of one deoxyhexose residue. These characteristic methyl group signals correlated in the HSQC spectrum of 1 with signals at δ_C 14.4 (C-18), 19.1 (C-19), 26.0 (C-26), 18.1 (C-27), and 11.8 (C-21), respectively. HMBC correlations with characteristic steroid methyl groups allowed for rapid assignment of the aglycone of 1 (Kuroda et al., 1999a). The HMBC correlations at δ_H/δ_C 2.65 (H-12)/68.1 (C-11) and 1.25 (H-9)/68.1 (C-11) indicated a secondary hydroxy function at C-11 (Fig. 2). The ¹H- and ¹³C-NMR spectral data of 1 (Table 1) showed chemical

^{*} Corresponding author.

^{**} Corresponding author.

E-mail addresses: pczhang@imm.ac.cn (P.-C. Zhang), jianqiangk@imm.ac.cn (J.-Q. Kong).

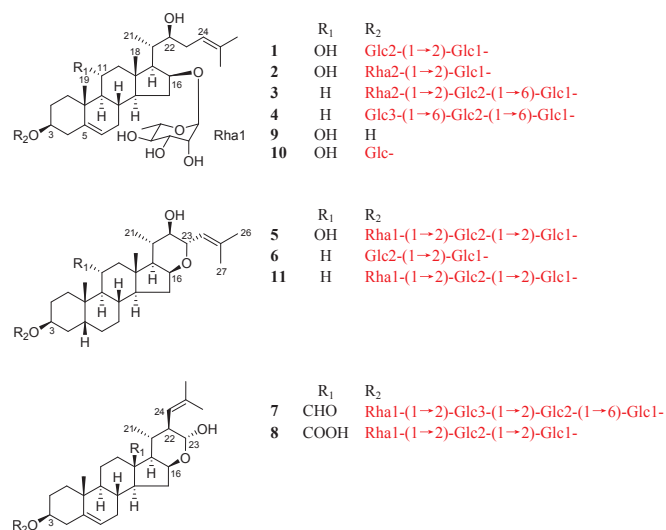


Fig. 1. Structures of compounds 1–11.

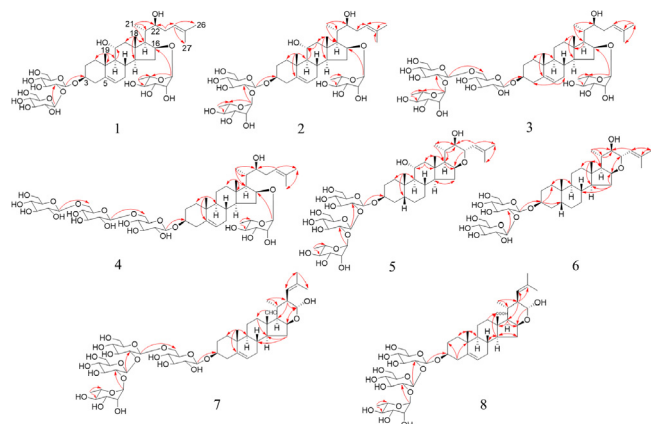


Fig. 2. Selected HMBC correlations of 1–8.

shifts in close agreement with those of known compound **10** (Iguchi et al., 2017a), which was assumed to possess the same planar steroidal skeleton, (22*S*)-cholesta-5,24-dien-3 β ,11 α ,16 β ,22-tetrol, as the aglycone, which was also confirmed by 2D NMR, including COSY, HSQC, and HMBC spectra.

The relative configuration of the aglycone moiety of **1** was demonstrated by a ROESY experiment (Fig. 3) and by comparing the NMR data of **1** with those of **10**. The ROESY correlations between H-19 β /H-1 β , H-2 β , H-4 β , and H-11 β indicated an α -OH at C-11. In addition, the correlations between H-1 α /H-3 α , H-9 α /H-14 α , H-14 α /H-17 α , and H-17 α /H-16 α allowed for assignment of β -OH at C-3 and C-16. Moreover, the ROESY cross-peaks at H-11 β /H-18 β , H-18 β /H-20 β , H-21 α /H-23 α , and H-23 α /H-22 α revealed the α -orientation of H-21 and a β -OH located at C-22. These data allowed for determination of the relative configuration of the aglycone fragment (Bie et al., 2019; Challinor et al., 2012).

The ¹H-NMR spectrum of **1** also contained signals typical of anomeric protons of a glycoside at δ_{H} 5.33 (d, J = 7.8 Hz, H-1 of Glc 2), δ_{H} 5.12 (d, J = 7.8 Hz, H-1 of Glc 1), and δ_{H} 5.27 (br s, H-1 of Rha 1), providing correlations in the HSQC spectrum with three anomeric carbon signals at δ_{C} 106.7, 101.4, and 105.0, respectively, indicating the presence of three sugar units. Correlations observed in the HMBC spectrum of **1** (Fig. 2) between the H-1 of Glc 2 at δ_{H} 5.33 and C-2 of Glc 1 at δ_{C} 84.8, H-1 of Glc1 at δ_{H} 5.12 and C-3 of the aglycone at δ_{C} 79.5, and H-1 of Rha 1 at δ_{H} 5.27 and C-16 of the aglycone at δ_{C} 82.2 established the presence of a (1 \rightarrow 2) linked diglucose moiety at position

Table 1

¹H NMR (600 MHz) and ¹³C NMR (150 MHz) data of compound **1** in C₅D₅N (δ in ppm, J in Hz).

Position	1		Position	1	
	δ_{C}	δ_{H}		δ_{C}	δ_{H}
1 α	39.6	1.33 m	3-O-Glc 1		
1 β		3.24 dd (14.4, 3.6, 3.6)	1	101.4	5.12 d (7.8)
2 α	30.5	2.22 m	2	84.8	4.19 q (9.0, 7.8)
2 β		2.04 m	3	78.0	4.40 m
3 α	79.5	3.95 m	4	71.4	4.31 m
4 α	39.9	2.92 m	5	78.2	4.29 m
4 β		2.89 m	6	62.8	4.64 br d (12.0)
5	141.9	–			4.53 br s
6	121.4	5.49 br d (5.4)		Glc 2	
7	32.2	1.97, 1.43 m	1	106.7	5.33 d (7.8)
8 β	31.7	1.90 m	2	77.1	4.18 q (9.0, 7.8)
9 α	57.1	1.25	3	77.9	4.05 m
10	38.8	–	4	71.5	4.30 m
11 β	68.1	4.29 m	5	78.8	3.92 m
12	51.8	2.65, 1.61 m	6	62.5	4.53 br s
13	43.0	–			4.39 m
14 α	54.5	1.02 s		16-O-Rha 1	
15 α	35.7	1.57 m	1	105.0	5.27 br s
15 β		2.32 m	2	72.6	4.52 br s
16 α	82.2	4.44 m	3	73.1	4.46 m
17 α	57.8	2.11 ddd (13.8, 7.2, 3.6)	4	74.0	4.32 m
18 β	14.4	1.02 s	5	71.0	4.28 m
19 β	19.1	1.43 s	6	18.4	1.73 d (5.4)
20 β	35.1	2.63 m			
21 α	11.8	1.28 d (7.2)			
22 α	72.0	4.12 m			
23 α	35.4	2.31 m			
23 β		2.62 m			
24	123.1	5.55 t (7.2)			
25	132.4	–			
26	26.0	1.69 s			
27	18.1	1.71 s			

C-3 and a single rhamnose residue at C-16. The sugars obtained by acid hydrolysis of **1** were identified as D-glucose and L-rhamnose by GC analysis of the trimethylsilyl-L-cysteine derivatives of the hydrolysates of **1** and authentic standards (t_{R} : 29.609 min, 23.551 min). The coupling constants of the anomeric protons at δ_{H} 5.33 (d, J = 7.8 Hz), δ_{H} 5.12 (d, J = 7.8 Hz), and δ_{H} 5.27 (br s) resulted in assignment of β - and α -configurations for the D-glucose and L-rhamnose moieties, respectively. These data implied that the structure of **1** was (22*S*)-3 β -[(β -D-glucopyranosyl-(1 \rightarrow 2)- β -D-glucopyranosyl)oxy]-11 α ,22-dihydroxycholesta-5,24-dien-16 β -yl α -L-rhamnopyranoside (Fig. 1).

HRESIMS analysis of osaundersioside B (**2**) resulted in an [M + Na]⁺ ion peak at m/z 909.4841 and an [M + H]⁺ ion peak at m/z 887.5031 (MW 886.4926, which corresponded to a molecular formula C₄₅H₇₄O₁₇). The ¹H- and ¹³C-NMR spectra of the aglycone of **2** confirmed that it was the same as the aglycone of compound **1**. The ¹H- and ¹³C-NMR spectra of **2** and **1** were closely related, with **1** only distinguished from **2** by the anomeric proton at δ_{H} 6.42 (br s) and the secondary methyl group at δ_{H} 1.81 (d, J = 6.5 Hz) (Table 2). The saccharide portion was characterized by extensive NMR experiments and GC analysis as one β -D-glucopyranosyl residue and two α -L-rhamnopyranosyl residues (t_{R} : 29.618 min, 23.558 min). The HMBC correlation at $\delta_{\text{H}}/\delta_{\text{C}}$ 6.42 (H-1, Rha 2)/77.6 (C-2, Glc 1) demonstrated that Rha 2 was located at C-2 of Glc 1, and $\delta_{\text{H}}/\delta_{\text{C}}$ 5.10 (H-1, Glc 1)/77.6 (C-3) confirmed that Glc 1 was located at C-3 of the aglycone. Another HMBC correlation at $\delta_{\text{H}}/\delta_{\text{C}}$ 5.27 (H-1, Rha 1)/81.8(C-16) demonstrated that Rha 1 was located at C-16 of the aglycone (Fig. 2). Thus, the structure of

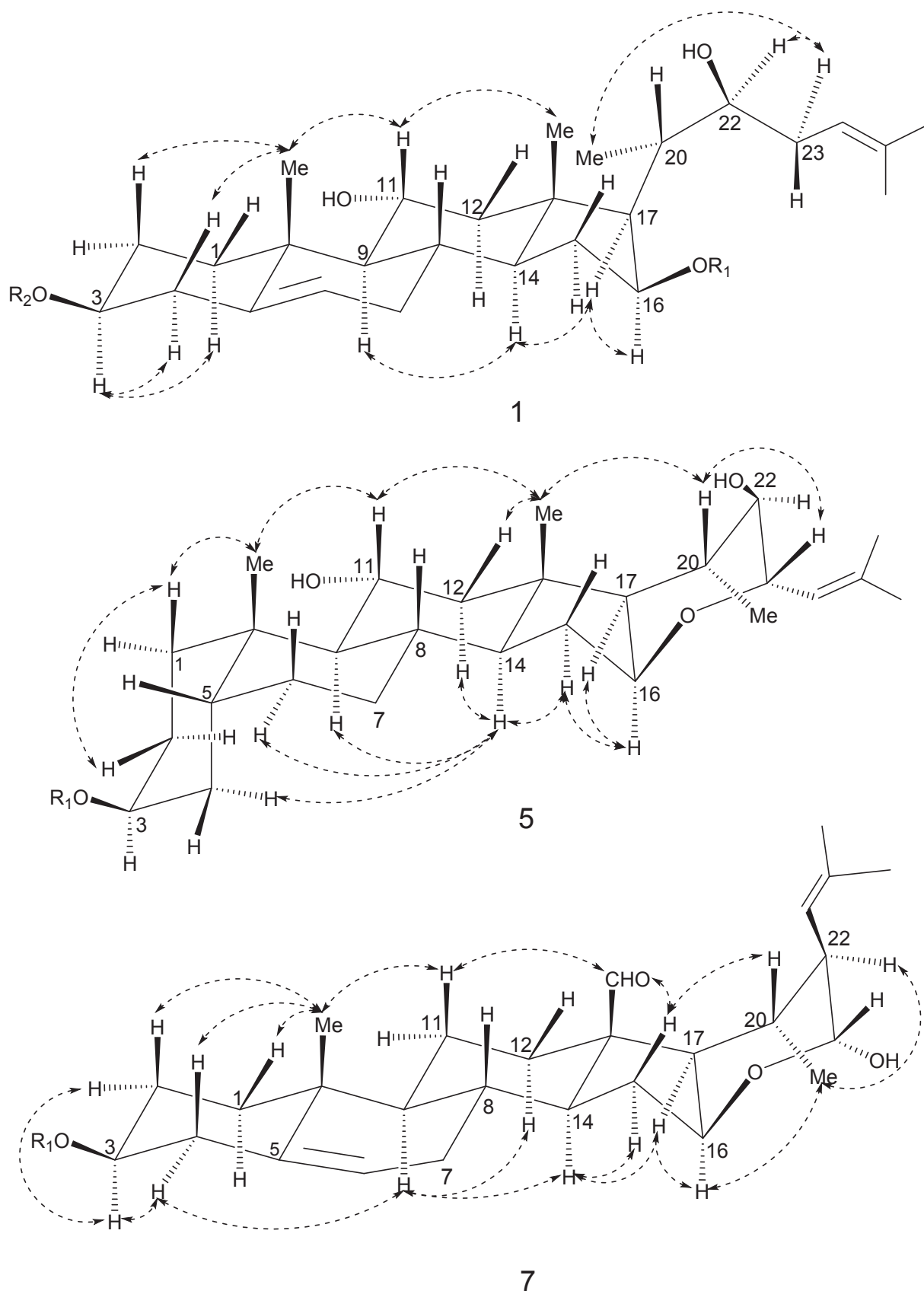


Fig. 3. Selected ROESY correlations of 1, 5 and 7.

Table 2

^1H NMR (500 MHz) and ^{13}C NMR (125 MHz) data of compound **2** in $\text{C}_5\text{D}_5\text{N}$ (δ in ppm, J in Hz).

Position	2	δ_{H}	Position	2	δ_{H}
	δ_{C}			δ_{C}	
1 α	38.9	1.38 m		3-O-Glc 1	
1 β		3.26 dd (14.0, 3.5, 3.5)	1	99.6	5.10 d (7.5)
2 α	29.8	2.18 m	2	77.6	4.33 m
2 β		2.12 m	3	79.0	4.34 m
3 α	77.6	4.06 m	4	71.1	4.21 m
4 α	39.0	2.91 m	5	77.2	3.92 m
4 β		2.11 m	6	61.9	4.53 br s
5	141.1	–			4.39 d (4.5)
6	120.9	5.43 br d (4.5)		Rha 2	
7	31.6	1.93, 1.49 m	1	101.4	6.42 br s
8 β	31.2	1.93 m	2	72.0	4.70 m
9 α	56.4	1.27 d (6.5)	3	72.2	4.46 m
10	38.3	–	4	73.6	4.40 m
11 β	67.5	4.33 m	5	68.8	5.09 m
12	51.1	2.65, 1.62 m	6	18.0	1.81 d (6.5)
13	42.3	–			
14 α	53.8	1.02 s		16-O-Rha 1	
15 α	35.0	1.64 m	1	104.4	5.27 br s
15 β		2.31 m	2	72.0	4.53 m
16 α	81.8	4.47 m	3	72.5	4.34 m
17 α	57.1	2.10 m	4	73.3	4.39 m
18 β	13.7	1.04 s	5	70.4	4.34 m
19 β	18.5	1.50 s	6	17.8	1.76 d (5.0)
20 β	34.5	2.62 m			
21 α	11.1	1.28 d (6.5)			
22 α	71.3	4.14 m			
23 α	34.7	2.31 m			
23 β		2.60 m			
24	122.4	5.52 t (6.0)			
25	131.7	–			
26	25.3	1.68 s			
27	17.4	1.70 s			

2 was (22*S*)-3 β -[[α -L-rhamnopyranosyl-(1 \rightarrow 2)- β -D-glucopyranosyl]oxy]-11 α ,22-dihydroxycholest-5,24-dien-16 β -yl α -L-rhamnopyranoside (Fig. 1).

Osaundersioside C (**3**) had a molecular formula of $\text{C}_{51}\text{H}_{84}\text{O}_{21}$ based on HRESIMS (m/z 1055.5354 [$\text{M} + \text{Na}$] $^+$, m/z 1033.5536 [$\text{M} + \text{H}$] $^+$, MW 1032.5505, positive-ion mode). Complete ^1H - and ^{13}C -NMR assignment of the steroidal skeleton of **3** demonstrated that this saponin contained an aglycone with a similar structure as that identified in **1** and **2** (Table 3). When the ^{13}C -NMR spectrum of **3** was compared with that of **1**, the hydroxymethine carbon signal observed at δ_{C} 68.1 (C-11) in the spectrum of **1** was displaced by a methylene carbon signal at δ_{C} 21.0 in that of **3**, and a set of signals corresponding to an additional terminal α -L-rhamnopyranosyl unit (Rha 2) (δ_{C} 102.0 (CH), δ_{C} 72.5 (CH), δ_{C} 72.8 (CH), δ_{C} 74.1 (CH), δ_{C} 69.5 (CH), and δ_{C} 18.7 (Me)) was observed (Kuroda et al., 2018). The ^1H -NMR spectrum showed the presence of four anomeric protons at δ_{H} 5.10 (d, $J = 15.0$ Hz), δ_{H} 4.97 (d, $J = 7.0$ Hz), δ_{H} 6.34 (br s), and δ_{H} 5.24 (br s), indicating the presence of four sugar units in **3**. The extensive 1D and 2D NMR experiments performed to evaluate **3**, and enantioselective GC analysis of the hydrolysate, showed the presence of two β -D-glucose units and two α -L-rhamnose units (t_{R} : 29.604 min, 23.542 min). Correlations were observed in the HMBC spectrum of **3** between δ_{H} 6.34 (H-1, Rha 2) and δ_{C} 77.4 (C-2, Glc 2), δ_{H} 5.10 (H-1, Glc 2) and δ_{C} 69.7 (C-6, Glc 1), δ_{H} 4.97 (H-1, Glc 1) and δ_{C} 78.4 (C-3, aglycone), and δ_{H} 5.24 (H-1, Rha 1) and δ_{C} 82.1 (C-16, aglycone) (Fig. 2). Thus, the structure of **3** was identified as (22*S*)-3 β -[[α -L-rhamnopyranosyl-(1 \rightarrow 2)- β -D-glucopyranosyl-(1 \rightarrow 6)- β -D-glucopyranosyl]oxy]-22-hydroxycholest-5,24-dien-16 β -yl α -L-rhamnopyranoside (Fig. 1).

HRESIMS analysis of osaundersioside D (**4**) resulted in a [$\text{M} + \text{Na}$] $^+$ ion peak at m/z 1071.5427, which resulted in a formula assignment of $\text{C}_{51}\text{H}_{84}\text{O}_{22}$ (MW 1049.5454). The ESIMS (positive-ion mode) spectrum

Table 3

^1H NMR (500 MHz) and ^{13}C NMR (125 MHz) data of compound **3** in $\text{C}_5\text{D}_5\text{N}$ (δ in ppm, J in Hz).

Position	3	δ_{H}	Position	3	δ_{H}
	δ_{C}			δ_{C}	
1 α	37.5	1.06 m		3-O-Glc 1	
1 β		1.75 m	1	100.6	4.97 d (7.0)
2 α	30.3	2.24 m	2	75.1	4.03 m
2 β		1.91 m	3	78.5	4.21 dd (7.0, 6.5)
3 α	78.4	3.92 m	4	71.6	4.22 dd (7.0, 6.5)
4 α	39.1	2.79 d (7.5)	5	76.9	3.99 m
4 β		2.65 m	6	69.7	4.77 br d (9.5)
5	140.9	–			4.31 m
6	121.8	5.43 br d (4.0)		Glc 2	
7	32.0	1.83, 1.41 m	1	105.4	5.10 br d (15.0)
8 β	31.8	1.83 m	2	77.4	4.13 m
9 α	50.2	0.84 m	3	79.5	4.13 m
10	36.9	–	4	71.5	4.11 m
11 α	21.0	1.29 dd (12.0, 2.0)	5	78.4	3.92 m
11 β		1.36 m	6	62.7	4.51 br s
12	39.9	1.98, 1.09 m			4.36 m
13	42.2	–		Rha 2	
14 α	54.8	0.77 m	1	102.0	6.34 br s
15 α	35.6	1.56 m	2	72.5	4.51 br s
15 β		2.29 m	3	72.8	4.32 m
16 α	82.1	4.38 m	4	74.1	4.33 m
17 α	57.7	1.99 m	5	69.5	4.99 m
18 β	13.1	0.91 s	6	18.7	1.78 d (6.0)
19 β	19.4	1.09 s			
20 β	35.4	2.31 m		16-O-Rha 1	
21 α	11.9	1.24 d (7.0)	1	105.0	5.24 br s
22 α	72.0	4.12 m	2	72.6	4.62 d (9.0)
23 α	35.1	2.31 m	3	73.1	4.43 m
23 β		2.61 m	4	73.9	4.32 m
24	123.5	5.54 m	5	71.0	4.31 m
25	132.2	–	6	18.4	1.71 d (5.0)
26	26.0	1.65 s			
27	18.1	1.68 s			

contained a [$\text{M} + \text{Na}-146$] $^+$ ion at m/z 925.4875, indicating the presence of a deoxyhexose unit. The ^1H - and ^{13}C -NMR spectral data confirmed **4** was a cholestane rhamnoside with similar spectrometric properties to those of **3**, as further demonstrated by HSQC and HMBC correlations. Compounds **4** and **3** differed by a mass of 16.0073, corresponding to one O atom, and the ^1H and ^{13}C signals associated with the sugar chain indicated three glucose units and one rhamnose unit (Table 4). The four sugars were determined to be three β -D-glucose units and one α -L-rhamnose unit in **4** using the procedures described above. In the HMBC spectrum of **4**, long-range correlations were observed between H-1 of Glc 3 at δ_{H} 5.06 (d, $J = 8.0$ Hz) and C-6 of Glc 2 at δ_{C} 69.9, between H-1 of Glc 2 at δ_{H} 5.06 (d, $J = 8.0$ Hz) and C-6 of Glc 1 at δ_{C} 69.9, between H-1 of Glc 1 at δ_{H} 4.96 (d, $J = 7.5$ Hz) and C-3 of the aglycone at δ_{C} 78.5, and between H-1 of Rha 1 at δ_{H} 5.23 (br s) and C-16 of the aglycone at δ_{C} 82.0 (Fig. 2). The structure of **4** was determined to be (22*S*)-3 β -[[β -D-glucopyranosyl-(1 \rightarrow 6)- β -D-glucopyranosyl-(1 \rightarrow 6)- β -D-glucopyranosyl]oxy]-22-hydroxycholest-5,24-dien-16 β -yl α -L-rhamnopyranoside (Fig. 1).

HRESIMS (positive-ion mode) analysis of osaundersioside E (**5**) resulted in peaks at m/z 925.4799 [$\text{M} + \text{Na}$] $^+$ and 903.5007 [$\text{M} + \text{H}$] $^+$ (MW 902.4875), consistent with the molecular formula $\text{C}_{45}\text{H}_{74}\text{O}_{18}$. The ^1H -NMR spectrum in pyridine- d_5 exhibited signals for two methyl groups at quaternary carbons at δ_{H} 1.09 (s, Me-18) and 1.30 (s, Me-19), two methyl groups on a double bond at δ_{H} 1.73 and 1.82 coupled to an olefinic proton at δ_{H} 5.83 (br d, $J = 7.5$ Hz), and one methyl group attached to a methine carbon at δ_{H} 1.37 (d, $J = 6.0$ Hz, Me-21) which correlated in the HSQC spectrum with five methyl carbons at δ_{C} 16.4 (C-18), 24.7 (C-19), 26.1 (C-26), 18.7 (C-27), and 17.4 (C-21), and one olefinic carbon at δ_{C} 125.9 (C-24). The presence of the quaternary carbon at δ_{C} 136.2 (C-25) was allowed for the existence of a double

Table 4¹H NMR (500 MHz) and ¹³C NMR (125 MHz) data of compound **4** in C₅D₅N (δ in ppm, J in Hz).

Position	4	δ _H	Position	4	δ _H
	δ _C			δ _C	
1α	37.4	1.07 m		3-O-Glc 1	
1β		1.73 m	1	102.8	4.96 d (7.5)
2α	30.4	2.26 m	2	75.0	4.10 m
2β		1.75 m	3	78.3	4.22 dd (9.0, 9.5)
3α	78.5	3.90 m	4	71.4	4.21 dd (9.0, 9.5)
4α	39.4	2.68 m	5	77.0	3.96 m
4β		2.47 m	6	69.9	4.96 d (7.5)
5	141.0	–			4.79 d (11.0)
6	121.7	5.31 br s		Glc 2	
7	31.9	1.85, 1.41 m	1	105.3	5.06 d (8.0)
8β	31.7	1.85 m	2	75.1	4.06 d (8.0)
9α	50.2	0.83 m	3	78.4	4.22 dd (9.0, 9.5)
10	36.8	–	4	71.4	4.21 dd (9.0, 9.5)
11α	21.0	1.30 dd (7.0, 7.0)	5	77.1	3.96 m
11β		1.36 m	6	69.9	4.85 d (13.5)
12	39.9	1.99, 1.09 m			4.79 d (11.0)
13	42.2	–		Glc 3	
14α	54.8	0.76 m	1	105.5	5.06 d (8.0)
15α	35.6	1.52 m	2	75.2	3.98 d (8.0)
15β		2.25 m	3	78.3	4.22 dd (9.0, 9.5)
16α	82.0	4.38 m	4	71.4	4.21 dd (9.0, 9.5)
17α	57.6	2.00 m	5	78.4	3.94 m
18β	13.1	0.89 s	6	62.5	4.50 br d (11.0)
19β	19.4	0.94 s			4.36 m
20β	35.1	2.28 m		16-O-Rha 1	
21α	11.8	1.24 d (6.5)	1	104.9	5.23 br s
22α	72.0	4.10 m	2	72.6	4.49 br d (11.0)
23α	35.4	2.30 m	3	73.1	4.42 m
23β		2.61 m	4	73.9	4.30 m
24	123.5	5.53 m	5	70.9	4.29 m
25	132.3	–	6	18.4	1.78 d (3.5)
26	25.9	1.65 s			
27	18.1	1.68 s			

Table 5¹H NMR (500 MHz) and ¹³C NMR (125 MHz) data compound **5** in C₅D₅N (δ in ppm, J in Hz).

Position	5	δ _H	Position	5	δ _H
	δ _C			δ _C	
1α	33.8	2.13 m		3-O-Glc 1	
1β		2.96 d (12.0)	1	101.2	5.05 d (7.5)
2α	28.7	2.04 m	2	78.2	4.61 m
2β		2.28 m	3	79.6	4.57 m
3α	75.3	4.40 m	4	71.8	4.13 m
4α	31.2	2.03 m	5	78.5	4.46 m
4β		2.00 m	6	63.6	4.57 m
5β	36.9	2.58 m			4.42 m
6α	27.5	1.91 m		Glc 2	
6β		1.59 m	1	101.8	5.91 d (7.0)
7	27.1	1.59, 1.18 m	2	79.9	4.23 m
8β	37.7	2.00 m	3	79.3	4.57 m
9α	47.4	1.79 d (10.0)	4	73.1	4.14 m
10	34.8	–	5	77.8	3.91 m
11β	68.1	4.18 m	6	62.5	4.48 m
12α	52.9	1.63 m			4.37 m
12β		2.52 s		Rha 1	
13	42.7	–	1	102.6	6.34 br s
14α	52.9	1.17 m	2	72.4	4.83 m
15α	34.5	2.18 m	3	72.7	4.69 m
15β		1.39 m	4	74.4	4.39 m
16α	72.5	4.35 m	5	69.6	5.05 d (7.5)
17α	60.2	1.25 dd (10.0, 7.5)	6	19.1	1.84 d (6.0)
18β	16.4	1.09 s			
19β	24.7	1.30 s			
20β	34.0	2.21 m			
21α	17.4	1.37 d (6.0)			
22α	76.4	3.58 m			
23β	77.8	4.62 m			
24	125.9	5.83 d (7.5)			
25	136.2	–			
26	26.1	1.73 s			
27	18.7	1.82 s			

bond, further supporting an open-chain steroidal aglycone. The ¹³C-NMR spectrum of **5** showed a total of 45 resonance lines, 18 of which were assigned to two glucose units and one rhamnose unit, and three anomeric carbons were observed at δ 102.6, 101.8, and 101.2. This implied a molecular formula of C₂₇H₄₄O₄ for the aglycone moiety, with 6 degrees of unsaturation, one of which was due to a double bond. Consequently, the aglycone of **5** was assumed to contain a C₂₇ steroid skeleton with a five-ring system (Table 5). On the basis of the aglycone structure, the ¹H- and ¹³C-NMR spectra of **5** were similar to those of **11** (Kuroda et al., 1997), with the exception that the chemical shift of C-11 (δ_C 68.1) was significantly downfield compared with C-11 (δ_C 22.0) in **11**, which was typical of hydroxylation. Moreover, the HMBC spectrum of **5** provided evidence that the hydroxyl group was located at C-11 of the aglycone moiety (Fig. 2).

The stereochemistry of the different ring junctions and substituents in **5** was determined via 2D ROESY. The ROESY correlations from H-19β/H-5β, H-14α/H-9α were consistent with A/B *cis* and B/C *trans* ring junctions. Cross-peaks observed from H-19β to H-1β, H-1β to H-2β, and H-3α to H-2α indicated β-orientation of the O-glycosyl moiety at C-3. Further ROESY signals for H-23β/H-20β, H-20β/H-19β, H-21α/H-22α/H-17α/H-16α/H-15α, H-15α/H-14α, and H-14α/H-12α confirmed C/D *trans* and D/E *cis* junctions, and 20S, 22R, and 23S configurations. Additional cross-peaks observed between H-19β and H-11β, and between H-18β and both H-11β and H-20β indicated the α-OH position at C-11 (Fig. 3).

The ¹H and 2D NMR data indicated a cholestane glycoside bearing a trisaccharide moiety attached to C-3 via an O-glycosidic linkage (Kicha et al., 2017). The sugars were identified by GC analysis as L-rhamnose and D-glucose (t_R: 29.632 min, 23.558 min). The coupling constants of the anomeric protons at δ_H 6.34 (br s), 5.05 (d, J = 7.5 Hz) and 5.91 (d,

J = 7.0 Hz) led to the assignment of α- and β-configurations for the L-rhamnose and D-glucose moieties, respectively. The HMBC correlations at δ_H/δ_C 6.34 (H-1, Rha 1)/77.6 (C-2, Glc 2), δ_H/δ_C 5.91 (H-1, Glc 2)/78.2 (C-2, Glc 1), and δ_H/δ_C 5.04 (H-1, Glc 1)/75.3 (C-3, aglycone) confirmed the linkage sequence of the trisaccharide moiety. These data were collectively used to determine the structure of **5** to be 3-[(α-L-rhamnopyranosyl-(1 → 2)-β-D-glucopyranosyl-(1 → 2)-β-D-glucopyranosyl)oxy]-16,23-epoxy-11α,22-dihydroxy-23-(2-methyl-1-propenyl)-(3β,16β,20S,22R,23S)-yl cholestane triglycoside (Fig. 1).

Osaundersioside F (**6**) had a molecular formula of C₃₉H₆₄O₁₃ based on HRESIMS (positive-ion mode, m/z 763.4253 [M + Na]⁺, MW 740.4347). The ¹H and ¹³C-NMR spectrometric data of **6** were analogous to those of **11**, and assignment of the aglycone signals of **6** via examination of COSY, HSQC, and HMBC spectra revealed that this saponin also contained the same structure as **11** (Table 6). Analysis of the sugars, as described above, revealed two β-D-glucose units (t_R: 29.568 min), and the NMR spectra exhibited the same attachment of a (1 → 2) linked diglucose moiety at C-3 of the aglycone as seen in **1** (Fig. 2). Therefore, the structure of **6** was determined to be 3-[(β-D-glucopyranosyl-(1 → 2)-β-D-glucopyranosyl)oxy]-16,23-epoxy-22-hydroxy-23-(2-methyl-1-propenyl)-(3β,16β,20S,22R,23S)-yl cholestane diglycoside (Fig. 1).

Osaundersioside G (**7**) was isolated as an amorphous solid. Its molecular formula of C₅₁H₈₀O₂₃ was deduced using HRESIMS (positive-ion mode, m/z 1083.5087 [M + Na]⁺, MW 1060.5090), indicating an index of hydrogen deficiency of 12. The IR spectrum was consistent with the presence of hydroxyl groups (3410 cm⁻¹) and an aldehyde group (1710 cm⁻¹); furthermore, the presence of the latter was further supported by ¹³C-NMR resonance at δ 207.4 (CHO). The ¹H-NMR spectrum of **7** displayed signals arising from three tertiary methyl

Table 6¹H NMR (500 MHz) and ¹³C NMR (125 MHz) data compound **6** in C₅D₅N (δ in ppm, J in Hz).

Position	6	δ _H	Position	6	δ _H
	δ _C			δ _C	
1α	30.7	1.48 m		3-O-Glc 1	
1β		1.83 m	1	101.9	4.97 d (7.5)
2α	27.0	1.51 m	2	83.0	4.27 m
2β		1.79 m	3	78.6	3.97 m
3α	75.2	4.31 m	4	71.7	4.19 t (9.0)
4α	30.9	1.83 m	5	78.2	4.19 t (9.0)
4β		1.80 m	6	62.8	4.57 m
5β	36.8	2.19 m			4.52 m
6α	26.8	1.95 m		Glc 2	
6β		1.50 m	1	106.0	5.41 d (7.5)
7	26.8	1.21, 1.16 m	2	77.7	4.26 m
8β	35.3	1.39 m	3	77.9	4.33 m
9α	40.2	1.29 m	4	71.5	4.34 m
10	35.2	–	5	78.2	3.88 m
11β	21.1	1.30, 1.21 m	6	62.6	4.52 m
12α	40.9	1.12 m			4.34 m
12β		1.86 s			
13	42.3	–			
14α	53.4	0.86 m			
15α	34.3	2.07 m			
15β		1.29 m			
16α	72.4	4.27 m			
17α	60.2	1.12 m			
18β	15.3	0.98 s			
19β	24.0	0.98 s			
20β	34.0	2.17 m			
21α	17.6	1.36 d (6.5)			
22α	76.4	3.59 br s			
23β	77.1	4.58 d (8.5)			
24	126.0	5.79 d (9.0)			
25	135.2	–			
26	26.1	1.69 s			
27	18.7	1.78 s			

groups at δ_H 0.76 (s, H₃-19), 1.68 (s, H₃-26), and 1.77 (s, H₃-27), and a secondary methyl group at δ_H 0.97 (d, *J* = 6.0 Hz, H₃-21) (Table 7). An olefinic carbon signal at δ_C 134.5 (C-25), an HSQC cross-peak at δ_H/δ_C 4.89 (m)/126.2 (C-24), and HMBC correlations between δ_H 4.89 (H-24) and both δ_C 26.0 (C-26) and 19.0 (C-27) suggested a Δ²⁴⁽²⁵⁾ double bond. An olefinic hydrogen signal at δ_H 5.35 (br s, H-6) correlated with the HSQC spectrum at δ_C 120.8, and a quaternary carbon at δ_C 141.2 (C-5) suggested a Δ⁵⁽⁶⁾ double bond. The signal at δ_H 10.11 (s) showed long range HMBC correlations with δ_C 33.5 (C-12), and 59.3 (C-13) was assigned to H-18. The HMBC correlations at δ_H/δ_C 2.44 (H-22)/59.4 (C-17)/98.2 (C-23), 5.12 (H-23)/69.7 (C-16), and 4.88 (H-16)/98.2 (C-23)/59.4 (C-17) indicated a six-membered hemiacetal ring between C-16 and C-23 (Fig. 2). The aglycone of **7** was identified as 16,23-epoxy-23-hydroxy-22-(2-methyl-1-propenyl)-24-norchole-5-en-18-al by comparison of its spectral data with those in the literature (Kuroda et al., 1999b), which had been previously isolated from the bulbs of *O. saundersiae* Baker.

The stereochemistry at the 3, 16, 20, 22, and 23 positions was determined by correlations in the ROESY spectrum. ROESY correlations between H-19β/H-8β, H-11β, H-18β/H-11β, H-15β, H-9α/H-14α, and H-15α/H-14α indicated that **7** had the usual B/C *trans* and C/D *trans* steroidal ring junctions. Other ROESY correlations between H-17α/H-21α, H-22α, H-16α, H-14α, H-15α/H-14α, H-17α, H-16α, H-22α/H-21α, H-17α, H-16α, H-16α/H-21α, H-17α, H-15α, H-22α, H-15β/H-20β, and H-20β/H-23β provided evidence of 20*S*, 22*S*, and 23*R* configurations. In addition, the ROESY cross-peaks at H-2α/H-3α and H-1α and H-4α/H-3α demonstrated the β-orientation of the *O*-glycosyl moiety at C-3 (Fig. 3).

For the saccharide portion, the ¹H-NMR spectrum of **7** exhibited four resonances in the deshielded region due to anomeric protons at δ_H

Table 7¹H NMR (500 MHz) and ¹³C NMR (125 MHz) data compound **7** in C₅D₅N (δ in ppm, J in Hz).

Position	7	δ _H	Position	7	δ _H
	δ _C			δ _C	
1α	37.5	1.06 dd (13.0, 11.0)		3-O-Glc 1	
1β		1.66	1	101.3	5.07 d (9.5)
2α	30.1	2.23 d (12.0)	2	75.2	4.25 m
2β		1.79 m	3	78.3	4.13 m
3α	78.4	3.93 m	4	71.5	4.76 m
4α	39.3	2.83 d (11.5)	5	76.7	3.98 m
4β		2.57 t (12.5)	6	69.8	5.01 m
5	141.2	–			4.88 m
6	120.8	5.35 br s		Glc 2	
7α	32.0	1.87 m	1	105.3	5.09 br s
7β		1.48 m	2	80.0	4.32 m
8β	33.4	1.62 m	3	79.4	4.33 m
9α	49.9	0.95 s	4	71.6	4.23 m
10	36.7	–	5	78.3	3.93 m
11α	22.5	1.37 m	6	62.6	4.51 m
11β		1.47 m			4.44 m
12α	33.5	2.63 br d (12.5)		Glc 3	
12β		1.00	1	102.0	5.86 m
13	59.3	–	2	78.5	4.23 m
14α	52.5	1.25 m	3	79.0	4.45 m
15α	33.4	2.34 ddd (7.5, 7.5, 6.0)	4	72.1	4.70 br d (9.0)
15β		1.94 m	5	77.8	3.99 m
16α	69.7	4.88 m	6	62.8	4.37 m
17α	59.4	1.45 m			4.31 m
18β	207.4	10.11 s		Rha 1	
19β	19.3	0.76 s	1	102.0	6.40 br s
20β	31.2	1.47 m	2	72.3	4.10 m
21α	18.6	0.97 d (6.0)	3	72.5	4.47 m
22α	47.5	2.44 ddd (10.5, 10.0, 7.5)	4	74.3	4.15 m
23β	98.2	5.12 br s	5	69.8	4.30 m
24	126.2	4.89 m	6	18.8	1.80 d (5.5)
25	134.2	–			
26	26.0	1.68 s			
27	19.0	1.77 s			

5.07 (br d, *J* = 9.5 Hz), 5.09 (br s), 5.86 (m), and 6.40 (br s) that correlated in the HSQC experiment with corresponding carbon signals at δ_C 101.3, 105.3, 102.0, and 102.0, respectively (Table 7). The β-pyranoid anomeric form of the glucose moieties was demonstrated by the large *J* value of the anomeric proton in the ¹H-NMR spectrum. A methyl doublet at δ_H 1.80 (d, *J* = 5.5 Hz) showed the presence of a 6-deoxyhexose unit. Acid hydrolysis of **7** resulted in three D-glucose and one L-rhamnose (*t_R*: 29.592 min, 23.530 min). Correlations in the HMBC spectrum of **7** between δ_H 6.40 (H-1, Rha 1) and δ_C 78.5 (C-2, Glc 3), δ_H 5.86 (H-1, Glc 3) and δ_C 80.0 (C-2, Glc 2), δ_H 5.09 and δ_C 69.8 (C-6, Glc 1), and δ_H 5.07 (H-1, Glc 1) and δ_C 78.4 (C-3, aglycone) established the presence of glycoside residues at position C-3 (Fig. 2). Thus, the structure of **7** was assigned as 3-[(α-L-rhamnopyranosyl-(1 → 2)-β-D-glucopyranosyl-(1 → 2)-β-D-glucopyranosyl-(1 → 6)-β-D-glucopyranosyl)oxy]-16,23-epoxy-23-hydroxy-22-(2-methyl-1-propenyl)- (3β,16β,20*S*,22*S*,23*R*)-24-norchole-5-en-18-al (Fig. 1).

The HRESIMS (positive-ion mode) spectrum of osaundersioside H (**8**) contained a peak at *m/z* 937.4488 [M + Na]⁺ (MW 914.4511), resulting in a molecular formula assignment of C₄₅H₇₀O₁₉. For the aglycone, the ¹H-NMR spectrum of osaundersioside H (**8**) exhibited signals corresponding to a tertiary methyl group, two secondary methyl groups, two methyl groups on a double bond, a hemiacetal proton, and two olefinic protons, which were analogous to those of **7** (Table 8), with the exception of one carboxylic carbon signal at δ_C 176.9 in **8** in place of the one aldehyde carbon signal at δ_C 207.4 in **7**. Correlations observed in the HMBC spectrum between δ_H 1.61 and δ_H 1.28 (H-12/14) and δ_C 176.9 (C-18) indicated a carboxyl group at C-13. As such, **8** was determined to be a C-18 carboxylic acid derivative of **7** for the aglycone

Table 8
 ^1H NMR (500 MHz) and ^{13}C NMR (125 MHz) data compound **8** in $\text{C}_5\text{D}_5\text{N}$ (δ in ppm, J in Hz).

Position	δ_{H}	Position	δ_{H}
δ_{C}		δ_{C}	
1 α	37.5	1.04 m	3-O-Glc 1
1 β	1.72 s	1	101.2
2 α	30.1	2.16 m	2
2 β	1.80 m	3	79.4
3 α	78.8	4.01 m	4
4 α	39.3	2.90 d (13.0)	5
4 β	2.62 m	6	62.7
5	141.2	–	
6	121.0	5.46 br s	Glc 2
7 α	33.0	2.61 m	1
7 β	2.51 m	2	102.2
8 β	32.5	2.35 m	2
9 α	50.6	1.10 m	3
10	37.1	–	4
11 α	23.7	1.73 m	5
11 β	1.77 m	6	62.9
12 α	32.4	2.08 m	
12 β	1.61 m	1	Rha 1
13	56.4	–	102.0
14 α	53.8	1.28 m	2
15 α	34.1	2.78 m	3
15 β	2.31 m	4	72.2
16 α	70.6	4.98 m	4
17 α	60.0	1.64 m	5
18 β	176.9	–	6
19 β	19.0	0.88 s	
20 β	32.5	2.09 m	
21 α	19.5	1.32 d (6.0)	
22 α	48.2	2.56 m	
23 β	98.3	5.27 d (6.5)	
24	127.0	5.03 m	
25	133.7	–	
26	26.0	1.71 s	
27	18.8	1.86 s	

moiety. Three anomeric proton signals were also present in the ^1H -NMR spectrum of **8**, and these displayed HSQC correlations with signals at δ_{C} 101.2 (Glc 1), 102.2 (Glc 2), and 102.0 (Rha 1). Correlations between δ_{H} 6.44 (s, H-1, Rha1) and δ_{C} 78.6 (C-2, Glc 2), δ_{H} 5.93 (d, $J = 7.5$ Hz, H-1, Glc 2) and δ_{C} 80.6 (C-2, Glc 1), and δ_{H} 5.18 (d, $J = 7.5$ Hz, Glc 1) and δ_{C} 78.8 (C-3, aglycone) in the HMBC spectrum of **8** revealed the presence of the same linked trisaccharide moiety observed in **5** and **11** (Fig. 2). Thus, **8** was assigned the structure 3-[(α -L-rhamnopyranosyl-(1 \rightarrow 2)- β -D-glucopyranosyl-(1 \rightarrow 2)- β -D-glucopyranosyl)oxy]-16,23-epoxy-23-hydroxy-22-(2-methyl-1-propenyl)-(3 β ,16 β ,20S,22S,23R)-24-norchol-5-en-18-oic acid (Fig. 1).

2.2. Cytotoxic activities of compounds 1–11

All isolates were evaluated for cytotoxic activity against five cell lines. Compound **3** exhibited specific cytotoxicity toward the MCF-7 cell line with an IC_{50} value of 0.20 μM , similar to that of the positive control, paclitaxel (19.9 nM). The IC_{50} values for compound **3** toward the other four cell lines were greater than 10 μM , it was thus considered to be inactive against these cells. Moreover, none of the other compounds exhibited cytotoxicity toward any of the cell lines, with IC_{50} values greater than 10 μM (Andriamisaina et al., 2019).

2.3. Anti-inflammatory activities of compounds 1–11

The *in vitro* anti-inflammatory activities of **1–11** were evaluated based on their abilities to inhibit LPS-induced NO production in mouse peritoneal macrophages. The results indicated that compound **8** inhibited NO production by 56.81% in macrophages at a concentration of

10^{-5} M. The other compounds were either inactive or only marginally active. The positive control DEX inhibited NO production by 97.23% at 10^{-5} M (Xiang et al., 2018).

3. Experimental

3.1. General experimental procedures

Optical rotation was measured using an Autopol V automatic polarimeter. UV spectra were obtained using a Jasco V650 spectrophotometer. IR spectra were recorded using a Nicolet 5700 FT-IR microscope transmission instrument. ^1H -NMR (500 or 600 MHz), ^{13}C -NMR (125 or 150 MHz), and 2D NMR spectrometric data were recorded using a Bruker AV-III-500 spectrometer or a Bruker-600 NMR spectrometer. Chemical shifts were reported in δ (ppm) with the solvent (pyridine- d_5) peaks as references. High-resolution electrospray ionization mass spectrometry (HRESIMS) was performed using an Agilent 6520 HPLC-Q-TOF (Agilent Technologies, Waldbronn, Germany). Preparative HPLC was performed using a SEP LC-52 instrument equipped with a SilGreen HPLC column (250 \times 10 mm, 5 μm , Peking, China). HPLC-DAD analysis was performed using an Agilent 1200 series system (Agilent Technologies) equipped with a COSMOSIL 5 C₁₈ MS-II column (250 \times 4.6 mm, 5 μm , Tokyo, Japan). Sephadex LH-20 (Pharmacia Fine Chemicals, Uppsala, Sweden), Diaion HP-20 (Mitsubishi Chemical Corp, Tokyo, Japan), silica gel (200–300 mesh, Qingdao Marine Chemical Factory, China), and ODS (50 μm , Merck, Germany) were used for column chromatography (CC). TLC was performed using precoated glass Si gel GF254 plates (Qingdao Marine Chemical Factory).

3.2. Plant material

The bulbs of *Ornithogalum saundersiae* Baker (Asparagaceae) were purchased from Yuanjiang County, Yunnan province, China in March 2015, and identified by Prof. Jian-Qiang Kong. A voucher specimen (OS-2015-03) was retained in our laboratory.

3.3. Extraction and isolation

The plant material (dry weight, 19.76 kg) was cut into small pieces and extracted with hot EtOH twice at 60 $^{\circ}\text{C}$. The EtOH concentrated *in vacuo* was partitioned with petroleum ether (3 \times 5 L), EtOAc (3 \times 5 L), and *n*-BuOH (3 \times 5 L). The *n*-BuOH layer was evaporated, and the residue (467 g) was separated using a Diaion HP-20 column (120 \times 20 cm) with a stepwise EtOH/H₂O mobile phase gradient (1:9 EtOH:H₂O v/v to 100% EtOH). Fractions eluted with 50% EtOH were further loaded onto an ODS silica gel column (46 \times 3.6 cm) under reduced pressure and eluted using a stepwise MeOH/H₂O gradient (1:9 MeOH/H₂O v/v to 100% MeOH) to yield 50% MeOH (22 g) and 60% MeOH (40 g) subfractions. The 50% MeOH subfraction was further separated using an LH-20 column (50 \times 10 cm) with a MeOH/H₂O stepwise gradient (1:4 MeOH/H₂O v/v to 100% MeOH), resulting in four fractions (I–IV). Fraction I was subjected to silica gel column chromatography and eluted with a stepwise CHCl₃/MeOH gradient (8:1–1:1, v/v) into 8 subfractions (I_a–I_h). Fraction I_c was separated using an ODS silica gel column (31 \times 2.6 cm) under reduced pressure with a stepwise MeOH/H₂O gradient (1:9–9:1, v/v) into fractions (I_{c,1}–I_{c,5}). Fraction I_{c,3} was subjected to silica gel column chromatography with a stepwise CHCl₃/MeOH/H₂O gradient (50:10:1–12:10:1, v/v), resulting in collection of 7 subfractions (I_{c,3,1}–I_{c,3,7}). Fraction I_{c,3,5} was submitted loaded onto a SilGreen C₁₈ column and eluted with 70% aqueous MeOH at 3 mL/min to obtain pure **3** (70.0 mg, t_{R} : 9.6 min). HPLC separation of Fraction I_{c,3,6} on a SilGreen C₁₈ column with MeOH/H₂O (17:8, v/v) at 3 mL/min yielded pure **4** (259.7 mg, t_{R} : 11.2 min) and **7** (265.7 mg, t_{R} : 14.5 min). Fraction I_g was separated by preparative HPLC (SilGreen C₁₈ column, 3 mL/min) using MeOH/H₂O

(2:1, v/v) to yield **1** (26.1 mg, t_R : 16.1 min) and **2** (104.2 mg, t_R : 20.4 min). HPLC separation of Fraction I_h using a SilGreen C₁₈ column (3 mL/min) with MeOH/H₂O (7:3, v/v) resulted in purification of **5** (256.8 mg, t_R : 13.4 min). A portion of Fraction II was purified using silica gel CC with CHCl₃/MeOH/H₂O (40:10:1–12:10:1) and a SilGreen C₁₈ column (3 mL/min) with MeOH/H₂O (2:1, v/v) to obtain **8** (17.7 mg, t_R : 15.3 min). The 60% MeOH fraction was separated on an ODS silica gel column (46 × 3.6 cm) under reduced pressure with a stepwise MeOH/H₂O gradient (1:9–100% MeOH, v/v), to yield 3 sub-fractions (A–C). Fraction B was separated by silica gel CC using CHCl₃/MeOH/H₂O (50:10:1–12:10:1, v/v/v) into 5 sub-fractions (B.1–B.5). HPLC separation of Fraction B.2 on a SilGreen C₁₈ column (3 mL/min) with MeOH/H₂O (13:7, v/v) yielded pure **6** (273.8 mg, t_R : 14.1 min).

3.4. Determination of the absolute configuration of sugar moieties

Determination of the absolute configurations of sugar moieties was performed as described previously (Shao et al., 2017). Compounds (**1–8**) (2 mg) were separately dissolved in 1M hydrochloric acid (2 mL) and refluxed for 12 h at 80 °C. The mixtures were concentrated under vacuum, and the residues were suspended in H₂O and extracted three times with ethyl acetate. The aqueous layers were evaporated under vacuum, diluted repeatedly with H₂O and evaporated under vacuum to produce neutral residues. The residues were dissolved in fresh anhydrous pyridine (1.0 mL). L-cysteine methyl ester hydrochloride (2 mg) was added, and the reaction mixtures were heated at 60 °C for 2 h. Then, the mixtures were concentrated under vacuum and placed in a drying oven for 2 h at 37 °C. N-trimethylsilylimidazole (0.2 mL) was added to the mixtures and heated at 60 °C for 2 h. H₂O (2 mL) was added to the mixtures to stop the reactions, and each mixture was extracted three times with *n*-hexane (2 mL each extraction). The *n*-hexane extracts were subjected to GC analysis under the following conditions: HP-5 (60 m × 0.25 mm, with a 0.25 μm film) column; FID detector; injector temperature of 300 °C; detector temperature of 300 °C; initial column temperature 200 °C, which was then raised to 280 °C at 8 °C/min, and the final temperature maintained for 30 min; N₂ as the carrier gas. D-glucose and L-rhamnose were confirmed by comparing the retention time of the derivatives of the purified molecules to the standard derivatized sugars, which had retention times of 29.662 min and 23.576 min, respectively.

3.5. Structural characterization

Osaundersioside A (**1**): Amorphous solid; [a]_D 20 – 27.8 (*c* = 0.9, MeOH); UV (MeOH) λ_{max} (log ϵ) 203.2 (4.07) nm; IR ν_{max} 3391, 2933, 1449, 1381, 1076, 1048, 633 cm⁻¹; ¹H-NMR (C₅D₅N, 600 MHz) and ¹³C-NMR (C₅D₅N, 150 MHz), see Table 1; HRESIMS (positive-ion mode) m/z 925.4797 [M + Na]⁺, m/z 903.4997 [M + H]⁺.

Osaundersioside B (**2**): Amorphous solid; [a]_D 20 – 60.0 (*c* = 1.3, MeOH); UV (MeOH) λ_{max} (log ϵ) 202.8 (3.94) nm; IR ν_{max} 3403, 2935, 1450, 1382, 1128, 1049, 637 cm⁻¹; ¹H-NMR (C₅D₅N, 500 MHz) and ¹³C-NMR (C₅D₅N, 125 MHz), see Table 2; HRESIMS (positive-ion mode) m/z 909.4841 [M + Na]⁺, m/z 887.5031 [M + H]⁺.

Osaundersioside C (**3**): Amorphous solid; [a]_D 20 – 38.2 (*c* = 1.1, MeOH); UV (MeOH) λ_{max} (log ϵ) 202.8 (3.98) nm; IR ν_{max} 3375, 2935, 1450, 1380, 1124, 1050, 625 cm⁻¹; ¹H-NMR (C₅D₅N, 500 MHz) and ¹³C-NMR (C₅D₅N, 125 MHz), see Table 3; HRESIMS (positive-ion mode) m/z 1055.5354 [M + Na]⁺, m/z 1033.5536 [M + H]⁺.

Osaundersioside D (**4**): Amorphous solid; [a]_D 20 – 46.7 (*c* = 0.9, MeOH); UV (MeOH) λ_{max} (log ϵ) 202.8 (3.93) nm; IR ν_{max} 3367, 3236, 2936, 1449, 1380, 1161, 1110, 629 cm⁻¹; ¹H-NMR (C₅D₅N, 500 MHz) and ¹³C-NMR (C₅D₅N, 125 MHz), see Table 4; HRESIMS (positive-ion mode) m/z 1071.5427 [M + Na]⁺.

Osaundersioside E (**5**): Amorphous solid; [a]_D 20 – 92.0 (*c* = 1.0, MeOH); UV (MeOH) λ_{max} (log ϵ) 203.2 (4.05) nm; IR ν_{max} 3376, 2926, 1449, 1378, 1126, 1073, 636 cm⁻¹; ¹H-NMR (C₅D₅N, 500 MHz) and

¹³C-NMR (C₅D₅N, 125 MHz), see Table 5; HRESIMS (positive-ion mode) m/z 925.4799 [M + Na]⁺, m/z 903.5007 [M + H]⁺.

Osaundersioside F (**6**): Amorphous solid; [a]_D 20 – 45.0 (*c* = 1.2, MeOH); UV (MeOH) λ_{max} (log ϵ) 203.4 (4.12) nm; IR ν_{max} 3375, 2927, 1449, 1377, 1076, 1047, 634 cm⁻¹; ¹H-NMR (C₅D₅N, 500 MHz) and ¹³C-NMR (C₅D₅N, 125 MHz), see Table 6; HRESIMS (positive-ion mode) m/z : 763.4253 [M + Na]⁺.

Osaundersioside G (**7**): Amorphous solid; [a]_D 20 – 65.0 (*c* = 1.0, MeOH); UV (MeOH) λ_{max} (log ϵ) 203.2 (4.14) nm; IR ν_{max} 3410, 2931, 1710, 1451, 1376, 1043, 636 cm⁻¹; ¹H-NMR (C₅D₅N, 500 MHz) and ¹³C-NMR (C₅D₅N, 125 MHz), see Table 7; HRESIMS (positive-ion mode) m/z 1083.5087 [M + Na]⁺.

Osaundersioside H (**8**): Amorphous solid; [a]_D 20 – 90.0 (*c* = 0.7, MeOH); UV (MeOH) λ_{max} (log ϵ) 202.8 (4.08) nm; IR ν_{max} 3402, 2932, 1710, 1444, 1376, 1072, 1034, 629 cm⁻¹; ¹H-NMR (C₅D₅N, 500 MHz) and ¹³C-NMR (C₅D₅N, 125 MHz), see Table 8; HRESIMS (positive-ion mode) m/z 937.4488 [M + Na]⁺.

3.6. Cytotoxicity assay

The cytotoxicity of compounds **1–11** against HCT-116 (human colon cancer cell line), HepG2 (human hepatocyte carcinoma cell line), BGC-823 (human gastric carcinoma cell line), A549 (human non-small-cell lung cancer cell line), and MCF-7 (human breast carcinoma cell line) cells was tested as described previously (Tang et al., 2013; Liu and Kong, 2018). Paclitaxel (10⁻⁵ M, final concentration) was used as the positive control.

3.7. Inhibition of LPS-induced NO production in macrophage

The inhibitory effects of compounds **1–11** on NO production in LPS-activated mouse peritoneal macrophages were evaluated according to an established procedure (Wang et al., 2014). Dexamethasone (DEX, 10⁻⁵ M, final concentration) was used as the positive control.

Conflicts of interest

The authors declare no conflict of interest.

Acknowledgments

This research was financially supported by the Drug Innovation Major Project (2018ZX09711001-006), CAMS Innovation Fund for Medical Sciences (CIFMS) (2016-I2M-3-012) and Beijing Natural Science Foundation (7172143).

References

- Andriamaisina, N., Mitaine-Offer, A.C., Miyamoto, T., Tanaka, C., Paululat, T., Lirussi, F., Lacaille-Dubois, M.A., 2019. Steroidal glycosides from *Ornithogalum dubium* houtt. *Phytochemistry* 160, 78–84.
- Bie, Q., Chen, C., Yu, M., Guo, J., Wang, J., Liu, J., Zhou, Y., Zhu, H., Zhang, Y., 2019. Dongtingnoids A-G: fusicoccane diterpenoids from a *penicillium* species. *J. Nat. Prod.* 82, 80–86.
- Challinor, V.L., Stuthe, J.M.U., Parsons, P.G., Lambert, L.K., Lehmann, R.P., Kitching, W., De Voss, J.J., 2012. Structure and bioactivity of steroidal saponins isolated from the roots of *Chamaelirium luteum* (False Unicorn). *J. Nat. Prod.* 75, 1469–1479.
- Hirano, T., Oka, K., Mimaki, Y., Kuroda, M., Sashida, Y., 1996. Potent growth inhibitory activity of a novel *Ornithogalum* cholestane glycoside on human cells: induction of apoptosis in promyelocytic leukemia HL-60 cells. *Life Sci.* 58, 789–798.
- Iguchi, T., Kuroda, M., Naito, R., Watanabe, T., Matsuo, Y., Yokosuka, A., Mimaki, Y., 2017a. Structural characterization of cholestane rhamnoses from *Ornithogalum saundersiae* bulbs and their cytotoxic activity against cultured tumor cells. *Molecules* 22, 1243–1264.
- Iguchi, T., Yokosuka, A., Kuroda, M., Mimaki, Y., 2017b. Cholestane glycosides from *Ornithogalum saundersiae* bulbs and their apoptosis-inducing activity via a mitochondria-independent pathway. *Planta Medica International Open* 4 Mo-PO-21.
- Kicha, A.A., Kalinovsky, A.I., Ivanchina, N.V., Malyarenko, T.V., Dmitrenok, P.S., Kuzmich, A.S., Sokolova, E.V., Stonik, V.A., 2017. Furostane series asterosaponins and other unusual steroid oligoglycosides from the tropical starfish *Pentaceraster regulus*. *J. Nat. Prod.* 80, 2761–2770.

- Kubo, S., Mimaki, Y., Terao, M., Sashida, Y., Nikaido, T., Ohmoto, T., 1992a. Acylated cholestane glycosides from the bulbs of *Ornithogalum saundersiae*. *Phytochemistry* 31, 3969–3973.
- Kubo, S., Mimaki, Y., Sashida, Y., Mikaido, T., Ohmoto, T., 1992b. New polyhydroxylated cholestane glycosides from the bulbs of *Ornithogalum saundersiae*. *Chem. Pharm. Bull.* 40, 2469–2472.
- Kuroda, M., Mimaki, Y., Sashida, Y., Nikaido, T., Ohmoto, T., 1993. Structure of a novel 22-homo-23-norcholestane trisaccharide from *Ornithogalum saundersiae*. *Tetrahedron Lett.* 34, 6073–6076.
- Kuroda, M., Mimaki, Y., Sashida, Y., Hirano, T., Oka, K., Dobashi, A., 1995. A novel 16, 23-epoxy-5 β -cholestane glycoside with potent inhibitory activity on proliferation of human peripheral blood lymphocytes from *Ornithogalum saundersiae* bulbs. *Chem. Pharm. Bull.* 43, 1257–1259.
- Kuroda, M., Mimaki, Y., Sashida, Y., Hirano, T., Oka, K., Dobashi, A., Hong-yu, Li, Harada, N., 1997. Novel cholestane glycosides from the bulbs of *Ornithogalum saundersiae* and their cytostatic activity on leukemia HL-60 and MOLT-4 cells. *Tetrahedron* 53, 11549–11562.
- Kuroda, M., Mimaki, Y., Sashida, Y., 1999a. Cholestane rhamnosides from the bulbs of *Ornithogalum saundersiae*. *Phytochemistry* 52, 445–452.
- Kuroda, M., Mimaki, Y., Sashida, Y., 1999b. Saundersiosides C-H, rearranged cholestane glycosides from the bulbs of *Ornithogalum saundersiae* and their cytostatic activity on HL-60 cells. *Phytochemistry* 52, 435–443.
- Kuroda, M., Mimaki, Y., Yokosuka, A., Sashida, Y., Beutler, J.A., 2001. Cytotoxic cholestane glycosides from the bulbs of *Ornithogalum saundersiae*. *J. Nat. Prod.* 64, 88–91.
- Kuroda, M., Kubo, S., Masatani, D., Matsuo, Y., Sakagami, H., Mimaki, Y., 2018. Aestivalosides A–L, twelve pregnane glycosides from the seeds of *Adonis aestivalis*. *Phytochemistry* 150, 75–84.
- Liu, M., Kong, J.Q., 2018. The enzymatic biosynthesis of acylated steroidal glycosides and their cytotoxic activity. *Acta Pharm. Sin. B* 8, 981–994.
- Malabed, R., Hanashima, S., Murata, M., Sakurai, K., 2017. Sterol-recognition ability and membrane-disrupting activity of *Ornithogalum* saponin OSW-1 and usual 3-O-glycosyl saponins. *Biochim. Biophys. Acta Biomembr.* 1859, 2516–2525.
- Mimaki, Y., Kuroda, M., Sashida, Y., Hirano, T., Oka, K., Dobashi, A., Koshino, H., Uzawa, J., 1996a. Three novel rearranged cholestane glycosides from *Ornithogalum saundersiae* bulbs and their cytostatic activities on leukemia HL-60 and MOLT-4 cells. *Tetrahedron Lett.* 37, 1245–1248.
- Mimaki, Y., Kuroda, M., Kameyama, A., Sashida, Y., Hirano, T., Oka, K., Koike, K., Nikaido, T., 1996b. A new cytotoxic cholestane bisdesmoside from *Ornithogalum saundersiae* bulbs. *Biosci. Biotechnol. Biochem.* 60, 1049–1050.
- Mimaki, Y., Kuroda, M., Kameyama, A., Sashida, Y., Hirano, T., Oka, K., Dobashi, A., Koike, K., Nikaido, T., 1996c. A new rearranged cholestane glycoside from *Ornithogalum saundersiae* bulbs exhibiting potent cytostatic activities on leukemia HL-60 and molt-4 cells. *Bioorg. Med. Chem. Lett.* 6, 2635–2638.
- Mimaki, Y., Kuroda, M., Kameyama, A., Sashida, Y., Hirano, T., Oka, K., Maekawa, R., Wada, T., Sugita, K., Beutler, J.A., 1997. Cholestane glycosides with potent cytostatic activities on various tumor cells from *Ornithogalum saundersiae* bulbs. *Bioorg. Med. Chem. Lett.* 7, 633–636.
- Shao, S.Y., Feng, Z.M., Yang, Y.N., Jiang, J.S., Zhang, P.C., 2017. Forsythenethosides A and B: two new phenylethanoid glycosides with a 15-membered ring from *Forsythia suspense*. *Org. Biomol. Chem.* 15, 7034–7039.
- Tang, Y., Li, N., Duan, J.A., Tao, W., 2013. Structure, bioactivity, and chemical synthesis of OSW-1 and other steroidal glycosides in the genus *Ornithogalum*. *Chem. Rev.* 113, 5480–5514.
- Wang, X.F., Zhang, Y., Lin, M.B., Hou, Q., Yao, C.S., Shi, J.G., 2014. Biomimetic synthesis of active isorhapontigenin dimers. *J. Asian Nat. Prod. Res.* 16, 511–521.
- Wojtkielewicz, A., Długosz, M., Maj, J., Morzycki, J.W., Nowakowski, M., Renkiewicz, J., Strnad, M., Swaczynová, J., Wilczewska, A.Z., Wójcik, J., 2007. New analogues of the potent cytotoxic saponin OSW-1. *J. Med. Chem.* 50, 3667–3673.
- Xiang, L.M., Wang, Y.H., Yi, X.M., He, X.J., 2018. Anti-inflammatory steroidal glycosides from the berries of *Solanum nigrum* L. (European black nightshade). *Phytochemistry* 148, 87–96.
- Yuan, S., Liu, M., Yang, Y., He, J.M., Wang, Y.N., Kong, J.Q., 2018. Transcriptome-wide identification of an aurone glycosyltransferase with glycosidase activity from *Ornithogalum saundersiae*. *Genes* 9, 327.